JVSTB
JOURNAL OF VACUUM SCIENCE AND TECHNOLOGY B

Growth and evolution of ZnCdSe quantum dots

C. X. Shan, X. W. Fan, J. Y. Zhang, Z. Z. Zhang, B. S. Li et al.

Citation: J. Vac. Sci. Technol. B **20**, 1102 (2002); doi: 10.1116/1.1481870
View online: http://dx.doi.org/10.1116/1.1481870
View Table of Contents: http://avspublications.org/resource/1/JVTBD9/v20/i3
Published by the AVS: Science & Technology of Materials, Interfaces, and Processing

Growth and evolution of ZnCdSe quantum dots

C. X. Shan,[a] X. W. Fan, J. Y. Zhang, Z. Z. Zhang, B. S. Li, Y. M. Lu, Y. C. Liu, D. Z. Shen, and X. G. Kong
Laboratory of Excited State Processes, Chinese Academy of Sciences, Changchun Institute of Optics, Fine Mechanics and Physics, No.1 Yan An Road, Changchun, 130021, People's Republic of China

X. H. Wang
Laboratory of Excited State Processes, Chinese Academy of Sciences, Changchun Institute of Optics, Fine Mechanics and Physics, No.1 Yan An Road, Changchun, 130021, People's Republic of China and National Key Laboratory of High Power Semiconductor Laser, Changchun Institute of Optics and Fine Mechanics, No.7 WeiXing Road, Changchun, 130022, People's Republic of China

(Received 2 October 2001; accepted 8 April 2002)

ZnCdSe quantum dots (QDs) were fabricated successfully under Stranski–Krastanow mode by metalorganic chemical vapor deposition. Prior to growth, the critical thickness was first calculated in terms of strain relaxation and the growth was then performed with the help of the calculation. The evolution of the QDs was also studied by atomic force microscopy and spectroscopy. Two kinds of variations in the QDs appeared over time, the Ostwald ripening process and dot-formation process. Moreover, the shape of the dots changed from pyramidlike to domelike, with the transition explained by the theory of crystal growth. By analyzing photoluminescence spectra, two emission mechanisms were revealed and were thought to be zero-dimensional (0D) and 2D-like excitons. With increasing growth interruptions, the luminescence intensity ratio of the 0D to 2D-like excitons increased, which gave further evidence of the evolution of QDs. © *2002 American Vacuum Society.* [DOI: 10.1116/1.1481870]

I. INTRODUCTION

Quantum dot (QD) structures have been a field of active research for the last few years because they are not only of basic physical interest but also of fundamental importance for many optoelectronic applications,[1] such as lasers and detectors. Thus, the study of the growth of QDs becomes not only interesting but also important. Several state-of-the-art methods have been applied to fabricate QD structures. Two important methods are high-resolution lithography combined with dry or wet etching[2,3] and growth on masked substrates.[4] Unfortunately, such processes inevitably deteriorate the quality of the crystal. Recent reports on the growth under Stranski–Krastanow mode offer possibilities for growing high-quality QD structures. However, since this growth mode needs a relatively large lattice mismatch, most attention has focused on Ge/Si[5] and group III–V systems, in particular, InAs embedded in GaAs,[6] which has a lattice mismatch of ~7%. The reports on group II–VI systems are mainly focused on the CdSe/ZnSe system, which is, in terms of strain relationships, identical to the well-established group III–V systems mentioned above.

Zhang *et al.* have grown ZnCdSe QDs on ZnSe (110) by molecular-beam epitaxy systems.[7] They grew a ZnSe/ZnCdSe/ZnSe heterostructure under growth conditions that could not lead to layer-by-layer growth of ZnSe. This ZnSe layer inevitably resulted in surface roughness and the ZnCdSe QDs then formed there. Therefore, in one sense, the growth was not done under SK mode. In this article, we discuss the growth of ZnCdSe QDs on substrates with relatively small mismatch (~3%) carried out by metalorganic chemical vapor deposition (MOCVD). The decrease in epitaxial mismatch increases the two-dimensional (2D) layer-by-layer region.[8] Thus, it is likely for the growth by MOCVD, in which it is difficult to control the growth rate very precisely. Previous to the growth, the critical thickness was calculated, then the growth of ZnCdSe QDs proceeded under the guidance of the calculated critical thickness. In addition, the QDs were monitored constantly by atomic force microscopy (AFM) after growth. In this way, the formation process of the QDs, which has rarely been reported, was seen clearly. The ripening process and the shape transition of the QDs was also observed by AFM measurement. Microphotoluminescence (micro-PL) spectra were employed to study the evolution, as well.

II. EXPERIMENT

The QD structures studied were prepared on GaAs (100) substrates by low-pressure MOCVD at 310 °C, with the growth pressure fixed at 24 Torr. The GaAs wafers were first cleaned by ultrasonator with a sequence of trichloroethylene, acetone, and ethanol for 5 min each. The substrates were then chemically polished in H_2SO_4:H_2O_2:H_2O=3:1:1 at 40 °C, and boiled in hydrochloric acid. After being loaded into the reaction chamber, the substrates were annealed at 600 °C in hydrogen ambient for 10 min to avoid gallium and arsenic oxide layers. Dimethylzinc (DMZn), dimethylcadmium (DMCd), and hydrogen selenide (H_2Se) were used as precursors. The flow rates of the three precursors, which were controlled by separate mass-flow controllers, were kept at 1.6×10^{-6}, 4.3×10^{-7}, and 5.5×10^{-6} mol /min, respectively. High purity hydrogen was used as carrier gas to carry

[a]Author to whom correspondence should be addressed; electronic mail: shen@public.cc.jl.cn

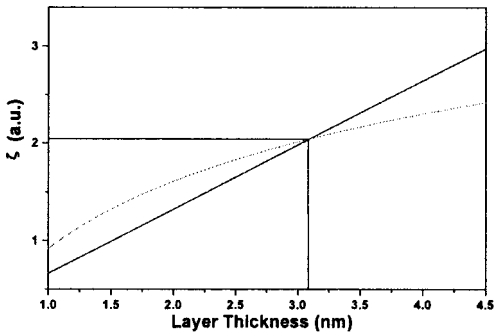

FIG. 1. Plot of the critical thickness of the $Zn_{0.56}Cd_{0.44}Se/GaAs$ system. The point of intersection yields the value.

the reactants into the reaction chamber. To avoid prereaction, the precursors were just mixed before the substrate. The typical growth rates for the ZnCdSe and ZnSe layers were 0.6 and 0.7 Å/s.

Two kinds of structures have been grown in our experiment: buried dots and exposed dots. For the buried dots, the ZnCdSe QDs were grown directly onto GaAs substrates. The exposed dots were intended for AFM studies. The buried dots contained a ZnSe buffer layer with a thickness of 170 nm. Following this is a five-period ZnCdSe/ZnSe system. The thicknesses of the ZnCdSe and ZnSe layers in this system were 3 and 14 nm, respectively. Finally, a 42 nm ZnSe cap layer terminates the structure. The buried dots are intended for photoluminescence measurement. Because the lattice mismatch of the CdSe/GaAs combination is 7%, which is close to that of the CdSe/ZnSe system (6.8%), the strain-induced self-organized QDs should be similar in both cases. Therefore, one can expect the exposed dots grown directly on the GaAs surface to be similar to the buried ones grown on ZnSe buffer layers.

For surface analysis, the exposed samples were monitored constantly at the same area by a Digital Instrument nanoscope IIIa system after being cooled down and taken out of the growth chamber. For PL measurement, the buried dots were excited by the 488 nm line of an Ar^+ laser, and the signals were measured by a Jobin-Yvon 630 micro-Raman spectrograph.

III. RESULTS AND DISCUSSION

A. Calculation of critical thickness

According to People and Bean,[9] the critical layer thickness of h_c vs lattice mismatch can be expressed by the following formula:

$$h_c \approx \left(\frac{1-\upsilon}{1+\upsilon}\right)\left(\frac{1}{16\pi\sqrt{2}}\right)\left[\frac{b^2}{a(x)}\right]\left[\left(\frac{1}{f^2}\right)\ln\left(\frac{h_c}{b}\right)\right], \tag{1}$$

where υ is Poisson's ratio, b is Bergers vector, $a(x)$ is the bulk lattice constant of the $Zn_{1-x}Cd_xSe$ layer, and f is the misfit parameter defined below:[10]

$$f = \frac{a_{\mathrm{ZnCdSe}} - a_{\mathrm{GaAs}}}{a_{\mathrm{GaAs}}} \tag{2}$$

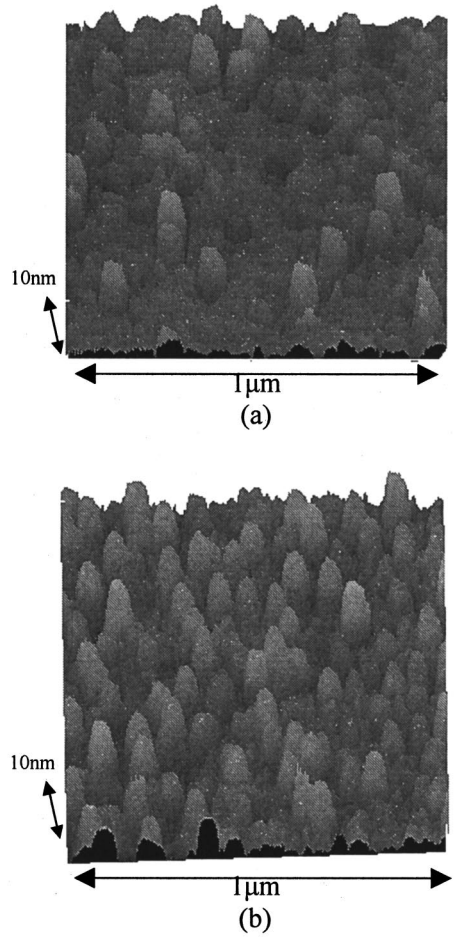

FIG. 2. AFM topologies of two ZnCdSe QD samples with different ZnCdSe coverage θ at the post-growth time of 120 min. (a) θ=2.5 nm and (b) θ=3.0 nm.

in which a_{ZnCdSe} and a_{GaAs} are the lattice constants of ZnCdSe and GaAs. Using the known constants of ZnSe, CdSe, and GaAs[11] and making a linear interpolation between ZnSe and CdSe, we find the lattice constant of $Zn_{0.56}Cd_{0.44}Se$ in our experiment to be 5.8359 Å. Based on Eq. (2), one can get f=0.032. Poisson's ratios of CdSe and ZnSe are 0.492 (Ref. 12) and 0.38,[13] respectively. The Poisson's ratio of $Zn_{0.56}Cd_{0.44}Se$, using the linear interpolation method, is found to be $\upsilon_{\mathrm{ZnCdSe}}$=0.429. As for the Burgers vector, it can usually be taken as b=4.008 Å.[10] Bringing all the known values into Eq. (1), one can get the following expression:

$$h_c = 15.1255 \ln\left(\frac{h_c}{4.008}\right). \tag{3}$$

Provide a variable ζ, so that

$$\zeta = \frac{h_c}{15.1255}. \tag{4}$$

One can plot Eq. (3) as shown in Fig. 1. From Fig. 1, we obtain the critical thickness of the ZnCdSe layer grown on GaAs is about 3.1 nm.

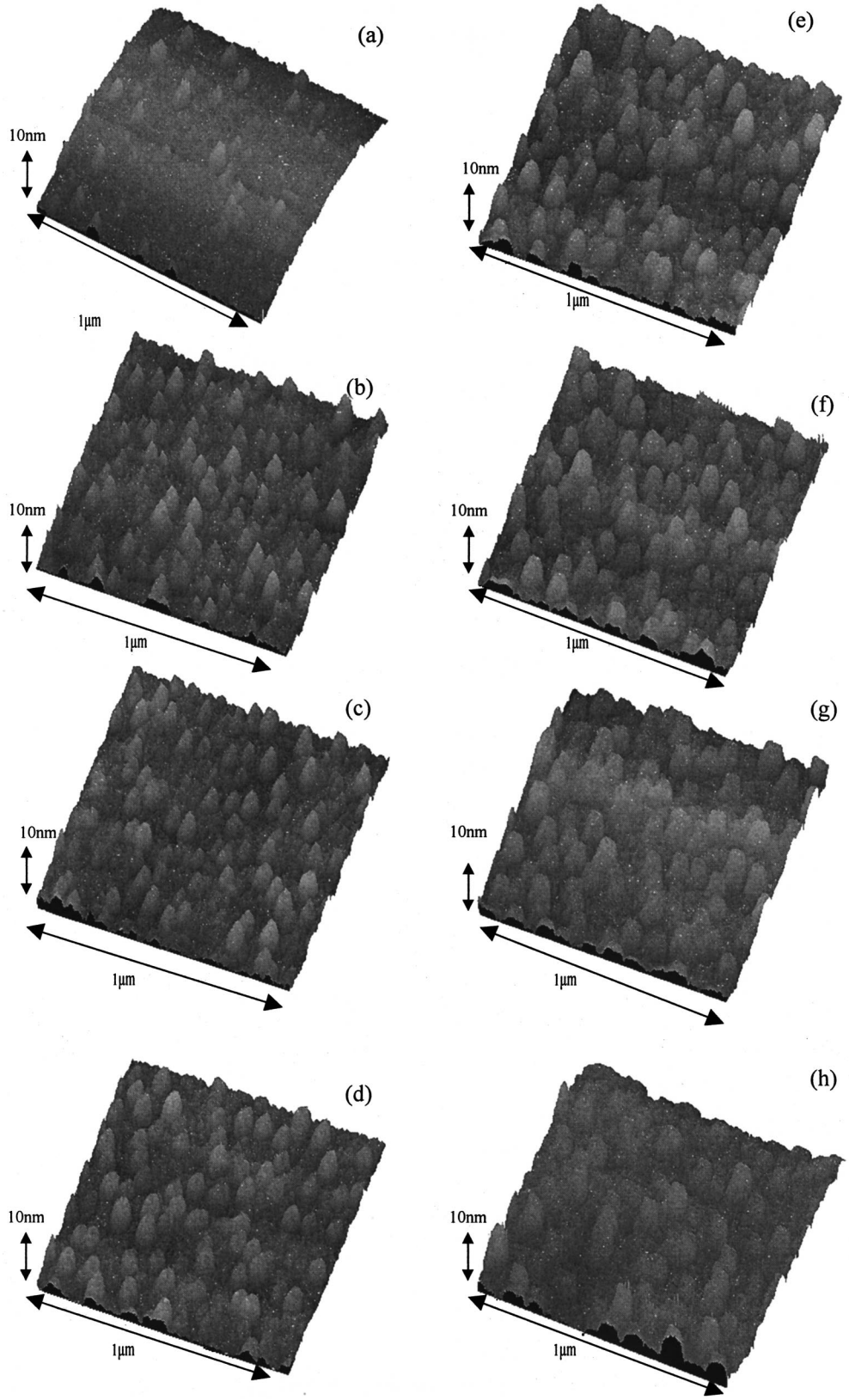

FIG. 3. AFM images of sample B at different postgrowth times: (a) 60; (b) 90; (c) 110; (d) 120; (e) 130; (f) 140; (g) 150; and (h) 180 min after growth.

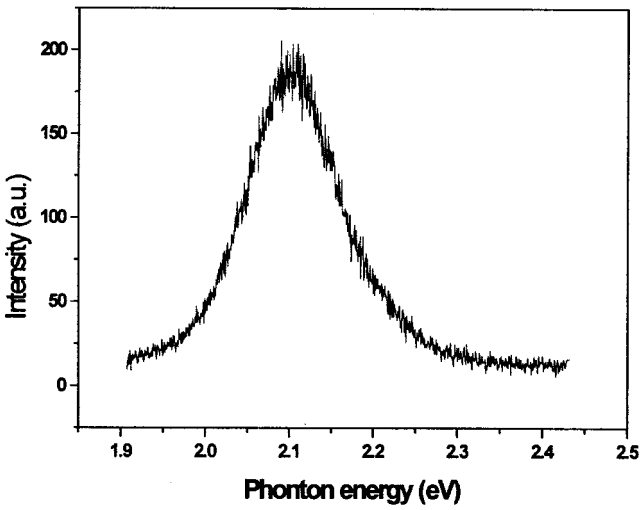

FIG. 4. Typical PL spectrum of ZnCdSe QD structure with 3 nm coverage and 300 s interruption at room temperature.

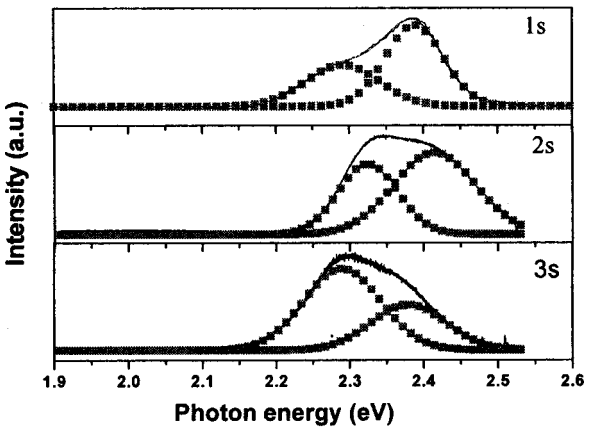

FIG. 5. Microphotoluminescence spectra taken at room temperature on a series of $Zn_{0.56}Cd_{0.44}Se/ZnSe$ QD samples with different growth interruptions. The dotted lines are the Gaussian simulations of the broad luminescence.

B. AFM studies of dot evolution

After the growth of several monolayers of ZnCdSe, the exposed samples were taken out of the growth chamber and monitored by AFM. Figure 2 shows the topologies of the two ZnCdSe QD samples with a ZnCdSe coverage of 2.5 and 3 nm. Note that both samples are below the calculated critical thickness, and both of the images were taken at 120 min after growth. What is surprising is that dots formed on both samples. Another phenomenon to note is that the density of sample A is much smaller than that of sample B. By calculating the number of dots in a typical 1 μm $\times$ 1 μm scanned area, the average density in Figs. 2(a) and 2(b) can be estimated to be about 20 and 100 μm^{-2}, respectively. The above phenomenon can be explained by the theory of surface diffusion.[14] When the coverage of the substrate is below the critical thickness, the diffusion of the surface atoms may result in parts of the sample surface reaching or exceeding the critical thickness, and then strain releases to form QDs. As for the density of the dots, the thicker the ZnCdSe coverage, the larger the strain energy, and therefore, more dots per unit area are required to release the strain energy,[15] as shown in Fig. 2.

The exposed dots in the same area were also monitored in air after being taken out of the growth chamber. Figure 3 displays such a sequence of AFM images of sample B. As is clear from the figures, the size of the dots increases monotonically, whereas the density varies in two stages. The first stage is from Figs. 3(a) to 3(d), and the second stage is from Figs. 3(e) to 3(h). In the first stage, the density increases from about 3×10^9 to 8×10^9 cm^{-2}, whereas in the second one, the density of the dots decreases gradually. We believe that the above phenomena are the combined effect of Ostwald ripening[16] and the formation of the dots led by diffusion. The formation of dots dominates the evolution in the first stage, so both the size and the density of the dots increase as time progresses. In the second stage, the Ostwald ripening process prevails over the formation process. Therefore, the size of the dots grows, but the density decreases with time. Besides the two above-mentioned processes, an interesting phenomenon in dot shapes with time occurs. In the initial stage, the shape of the dots appears pyramid-like, whereas in the final stage, the dots are shaped dome-like. According to the theory of crystal growth,[17] the surface of a concave area possesses lower surface vapor pressure (higher surface binding energy), and the surface of a convex area possesses higher surface vapor pressure (lower surface binding energy). Therefore, individual atoms or molecules continually migrate from the convex area to the concave area or less convex area. Moreover, as atoms arrive on the surface and diffuse to the island, they tend to stick to the concave area. Consequently, the dots become less acicular over time.

C. Spectroscopic studies of dot evolution

Figure 4 shows the typical PL spectrum of a ZnCdSe QD structure with 3 nm coverage and 300 s interruption between dot formation and capping at room temperature. As one can see, the full width at half-maximum (FWHM) of ZnCdSe QDs is about 120 meV, which is much larger than that of CdSe QDs, which are reported to be about 80 meV by several groups.[18–20] The broadening of the FWHM in our sample is largely due either to the size distribution of quantum dots or to the fluctuation in the ZnCdSe alloy. To study the evolution of the QDs by spectroscopy, we have also prepared three other buried samples with the growth-interruption time ranging from 1 to 3 s. The micro-PL spectra of these samples recorded at room temperature are shown in Fig. 5. The most remarkable feature in the spectra is the asymmetry of the broad PL lines. We can model the luminescence spectra as a superposition of two Gaussian lines. Dotted curves in Fig. 5 show two-line fits to the data, which provide a good description of the PL line shape observed in our samples. According to Kim *et al.*,[21] the line shape on the low-energy side is associated with QDs or zero-dimensional excitons, whereas the line shape on the high-energy side is the emission from more-extended regions that are two-

dimensional (2D) in character. As seen in Fig. 5, the intensity ratio of the low-energy line to the high-energy line increases with increasing interruption duration. This can be interpreted as follows. When the deposited material is below the critical thickness, the ZnCdSe layers are 2D-like, but over time, more area can reach the critical thickness and form QD structures by the effect of diffusion described above. Therefore, the emission from QDs becomes stronger, whereas that from 2D excitons decrease with increased interruption duration. Comparing the spectra in Fig. 4 with that in Fig. 5, one can find that the line shape in Fig. 4 redshifts significantly, which can be interpreted by virtue of the quantum confinement effect. With increasing interruption duration, the size of the dot becomes greater, as shown in Fig. 3. Thus, the quantum confinement effect weakens, and the PL spectra redshifts. The relative intensity variation and the redshift of the emission spectra verify to some degree the evolution of QDs revealed directly by the AFM study depicted above.

IV. CONCLUSIONS

In summary, ZnCdSe QDs have been grown based on the calculated critical thickness by MOCVD. The evolution of the QDs was studied by AFM. The size of the dots grows larger monotonically over time, whereas the density first increases and then gradually decreases, which are the combined effect of the Ostwald ripening and the dot-formation process. Another evolution of the dots is in shape changes from pyramidlike to domelike, which is interpreted by the theory of crystal growth. Two emission peaks appear in the PL spectra and are thought to be the emission of 0D- and 2D-like excitons. With increasing growth interruptions, the PL intensity ratio of the 0D to 2D excitons increases, verifying the evolution process revealed directly by AFM.

ACKNOWLEDGMENTS

This article was supported by the National Fundamental and Applied Research Project; the Key Project of the National Natural Science Foundation of China, No. 69896260; the Innovation Project Item, Chinese Academy of Sciences; the Program of CAS Hundred Talents; and the National Natural Science Foundation of China.

[1]D. L. Huffaker, G. Park, Z. Zou, O. B. Shchukin, and D. G. Deppe, Appl. Phys. Lett. **73**, 2564 (1998).
[2]K. Kash, A. Scherer, J. M. Worlock, H. G. Craighead, and M. C. Tamargo, Appl. Phys. Lett. **49**, 1043 (1986).
[3]M. Kohl, D. Heltmann, P. Grambow, and K. Ploog, Phys. Rev. B **41**, 2110 (1990).
[4]T. Fukui, H. Saito, M. Kasu, and S. Ando, J. Cryst. Growth **124**, 493 (1992).
[5]G. Capellini, L. Di Gaspare, F. Evangelisti, and E. Palange, Appl. Phys. Lett. **70**, 493 (1997).
[6]Ch. Heyn, D. Endler, K. Zhang, and W. Hansen, J. Cryst. Growth **210**, 421 (2000).
[7]B. P. Zhang, T. Yasuda, Y. Segawa, H. Yaguchi, K. Onabe, E. Edamatsu, and T. Itoh, Appl. Phys. Lett. **70**, 2413 (1997).
[8]G. S. Solomon, J. A. Trezza, and J. S. Harris, Jr., Appl. Phys. Lett. **66**, 991 (1995).
[9]R. People and J. C. Bean, Appl. Phys. Lett. **47**, 322 (1985).
[10]K. Pinardi, Uma Jain, S. C. Jain, H. E. Maes, R. Van Overstraeten, and M. Willander, J. Appl. Phys. **83**, 4724 (1997).
[11]B. L. Sharma and R. K. Purohit, *Semiconductor Heterojunctions* (Pergamon, New York, 1974), p. 24.
[12]C. F. Cline, H. L. Dunegan, and G. W. Henderson, J. Appl. Phys. **38**, 1944 (1967).
[13]T. Yokogawa, M. Ogura, and T. Kajiwara, J. Appl. Phys. **62**, 2843 (1987).
[14]Y. Yang, D. Z. Shen, J. Y. Zhang, X. W. Fan, Z. H. Zhen, X. W. Zhao, D. X. Zhao, and Y. N. Liu, J. Cryst. Growth **225**, 431 (2001).
[15]Z. H. Ma, W. D. Sun, I. K. Sou, and G. K. L. Wong, Appl. Phys. Lett. **73**, 1340 (1998).
[16]M. Zinke-Allmang, L. C. Feldman, and M. H. Grabow, Surf. Sci. Rep. **16**, 377 (1992).
[17]B. R. Pamplin, *Crystal Growth* (Pergamon, Oxford, 1975), p. 15.
[18]S. H. Xin, P. D. Wang, A. Yin, C. Kim, M. Dobrowolska, J. L. Merz, and J. K. Furdyna, Appl. Phys. Lett. **69**, 3884 (1996).
[19]M. Rabe, M. Lowisch, and F. Henneberger, J. Cryst. Growth **184/185**, 248 (1998).
[20]J. L. Merz, S. Lee, and J. K. Furdyna, J. Cryst. Growth **814/185**, 228 (1998).
[21]C. S. Kim, M. Kim, S. Lee, J. K. Furdyna, M. Dobrowolska, H. Rho, L. M. Smith, and H. E. Jackson, J. Cryst. Growth **214/215**, 761 (2000).